Inorg. Chem. **2004**, *43*, 3242–3247

Synthesis of $[NH_4]MnCl_2(OAc)$ and $[NH_4]_2MnCl_4(H_2O)_2$ by Solvothermal Dehydration and Structure/Property Correlations in a One-Dimensional Antiferromagnet

James D. Martin,* Ryan F. Hess, and Paul D. Boyle

Department of Chemistry, North Carolina State University, Raleigh, North Carolina 27695-8204

Received January 29, 2004

The utility of the solvothermal dehydration strategy whereby superheated acetonitrile reacts with water of hydration to form ammonium acetate is demonstrated in the synthesis of $[NH_4]MnCl_2(OAc)$, **I**, and $[NH_4]_2MnCl_4(H_2O)_2$, **II**, from $MnCl_2 \cdot 4H_2O$. The structure of **I** is shown to crystallize in the monoclinic space group *C*2/*c* (No. 15) with $a = 15.191(6)$ Å, $b = 7.044(2)$ Å, $c = 13.603(6)$ Å, $\beta = 107.31°$, $V = 1389.7(9)$ cm^{-1}, and $Z = 8$. The structure of **II** crystallizes in the space group *I*4/*mmm* (No. 139) with $a = 7.5250(5)$ Å, $b = 8.276(2)$ Å, $V = 468.6(1)$ cm^{-1}, and $Z = 2$. Both structures exhibit extensive hydrogen bonding that controls both local Mn–Cl bonding and the interchain organization. **I** is shown to be a one-dimensional Heisenberg antiferromagnet with an intrachain exchange constant $J/k = -2.39$ K. This structure exhibits exchange coupling intermediate between the well-studied triply and doubly chloride-bridged one-dimensional manganese Heisenberg antiferromagnets. The structure/property correlation demonstrates a linear dependence of the exchange constant on the Mn–Cl–Mn bond angle, α, for $\alpha < 94°$.

Introduction

Their unique electrochemical and magnetic properties have stimulated extensive investigation of the chemistry of manganese compounds ranging from biological molecules to advanced materials applications. Numerous complexes with carboxylate and amine ligands have been studied to model the active center of photosystem II.[1,2] Accessible oxidation states with up to five unpaired electrons per metal center have been exploited to prepare complexes with multiple manganese centers resulting in very high spin molecules. These molecules have provided the first demonstration of single-molecule magnets.[3] Langmuir−Blodgett films of manganese stearate provided the first demonstration of two-dimensional magnets.[4] Also lithium manganates are under considerable exploration as cathode materials for rechargeable lithium-ion batteries.[5] In our continuing development of the design and synthesis of metal−halide framework materials, we have begun to investigate syntheses with spin-rich and electroactive manganese chlorides. The solvothermal reaction of $MnCl_2 \cdot 4H_2O$ in acetonitrile, reported here, highlights solvothermal dehydration as a useful synthetic strategy and yields a new one-dimensional Heisenberg antiferromagnet that provides important insight into structure/property correlations of ligand bridges that control magnetic superexchange through ligand bridges.

Experimental Section

General Procedures. Reagents and solvents were purchased from Aldrich and Fisher. Solids were used as received, and moisture was removed from the acetonitrile by storing it over 4 Å molecular sieves. Characterization by X-ray powder diffraction was performed using an Enraf-Nonius Guinier camera. Single-crystal diffraction data were collected using an Enraf-Nonius CAD4-MACH diffractometer. Elemental analysis was performed by Atlantic Microlab Inc.

Synthesis. *Caution! Solvothermal reactions generate significant pressures when heated, which can lead to vessel rupture. Appropriate shielding should be utilized such as placing the thick-walled (2 mm) fused-silica reaction tubes in a capped iron pipe during heating.*

$[NH_4]MnCl_2(OAc)$, I. A total of 300 mg (1.48 mmol) of $MnCl_2 \cdot 4H_2O$ was placed in a thick-walled (12 mm o.d. × 8 mm i.d.) fused-

* Author to whom correspondence should be addressed. E-mail: jdmartin@ncsu.edu.

(1) Christou, G. *Acc. Chem. Res.* **1989**, *22*, 328.
(2) Wieghardt, K. *Angew. Chem., Int. Ed. Engl.* **1989**, *28*, 1153.
(3) Yoo, J.; Brechin, E. K.; Yamaguchi, A.; Nakano, M.; Huffmann, J. C.; Maniero, A. L.; Brunel, L.-C.; Awaga, K.; Ishimoto, H.; Christou, G.; Hendrickson, D. N. *Inorg. Chem.* **2000**, *39*, 3615 and references therein.
(4) Pomerantz, M.; Dacol, F. H.; Segmüller, A. *Phys. Rev. Lett.* **1978**, *40*, 246.
(5) Armstrong, A. R.; Bruce, P. G. *Nature* **1996**, *381*, 499.

10.1021/ic049881r CCC: $27.50
Published on Web 04/15/2004

silica tube, into which 3 mL of acetonitrile was then added. The reaction mixture was frozen in liquid N_2, and the reaction tube was flame sealed to 10 cm for a 60% fill by volume. The reaction was then placed in an oven at 150 °C for 8 days. Several large pink swordlike crystals (2 mm × 1 mm × >10 mm) as well as smaller needle crystals of **I** were obtained (>60% yield) along with as yet unidentified colorless and peach-colored powders. Elem anal. Calcd for crystals of **I**, $C_2H_7NCl_2O_2Mn$: C, 10.48; H, 3.08; N, 6.90. Found: C, 9.66; H, 3.65; N, 7.55. IR data (cm^{-1}): 3403 (s), 3182 (s), 1654 (m), 1560 (s), 1405 (m), 1048 (w), 1024 (w), 791 (w), 664 (m).

$[NH_4]_2MnCl_4 \cdot 2H_2O$, II. In related reactions with poly(carboxylic acid)s, such as oxalic acid and 1,3,5-triazine, using the synthesis conditions above, crystals of **I** (about 50%) were observed, identified by powder X-ray diffraction, along with small colorless crystals of **II** (about 15%), identified by single-crystal X-ray diffraction. The balance of the material, about 35%, was an as yet unidentified colorless microcrystalline material that based on elemental analysis is anticipated to be a poly(carboxylic acid)-containing material.

Single-Crystal X-ray Diffraction. All crystals were coated in Apiezon grease under a nitrogen atmosphere and mounted in Pyrex capillaries. Single-crystal measurements were performed at room temperature using a CAD-4 diffractometer with monochromatic Mo Kα radiation. Data were reduced and refined using the NRCVAX suite of programs.[6]

$[NH_4]MnCl_2(OAc)$, I. A pink single crystal (0.40 × 0.15 × 0.15 mm) was cleaved from a larger crystal for the diffraction measurement. Lattice constants were determined by a symmetry-constrained fit of 24 well-centered reflections between $30° < 2\theta < 63°$ and their Friedel pairs. Data were initially collected in a triclinic setting; however, examination of the Laue symmetry clearly revealed monoclinic symmetry. A unique quadrant of data, $\pm h, k, l$, was collected using the ω scan mode with 2440 independent reflections, $2\theta < 50°$. The data were scaled to three intensity check reflections using a five-point smoothing routine. An empirical absorption correction was applied using ψ-scan data.

The structure was initially solved using SIR92 in the *Cc* space group. However, this solution indicated a higher symmetry consistent with the space group *C*2/*c*. After the cell was transformed to *C*2/*c*, DIRDIF was used to position the asymmetric unit correctly with regard to the crystallographic centers of symmetry. All non-hydrogen positions were located by direct methods and refined using anisotropic displacement parameters. The ammonium hydrogens were then located in a subsequent difference Fourier map and idealized to N−H = 0.86 Å. The acetate hydrogens were introduced into idealized positions with C−H = 0.96 Å. A full-matrix least-squares calculation on 1025 unique reflections [$I > 1\sigma$] was used in the final refinement. Final residuals of $R = 0.041$ and $R_w = 0.047$ were obtained.

$[NH_4]_2MnCl_4 \cdot 2H_2O$, II. A colorless single crystal (0.20 × 0.15 × 0.10 mm) was selected for the diffraction measurement. Lattice constants were determined by a symmetry-constrained fit of 24 well-centered reflections between $23° < 2\theta < 35°$ and their Friedel pairs. A unique octant of data, *h*, *k*, *l*, was collected using the ω scan mode with 250 independent reflections, $2\theta < 50°$. The data were scaled to three intensity check reflections using a five-point smoothing routine.

Systematic absences were consistent with the *I*4/*mmm* space group, which was confirmed in the subsequent refinement. The non-hydrogen atoms of the isomorphous $K_2MnCl_4 \cdot 2H_2O$ structure[7] were used as the starting trial structure. All non-hydrogen atoms were allowed to be refined using anisotropic displacement parameters. Approximate hydrogen positions were obtained from a Fourier difference map and then idealized (O,N−H = 0.86 Å) with respect to their parent O or N atoms. A full-matrix least-squares calculation on 120 unique reflections [$I > I\sigma$] was used in the final refinement. Final residuals of $R = 0.040$ and $R_w = 0.049$ were obtained.

Magnetic Susceptibility. Magnetic susceptibility measurements were performed on an 11 mg sample of powdered single crystalline $[NH_4]MnCl_2(OAc)$, **I**, loaded into a fused-silica container with the sample held between two fused-silica rods. Data were obtained over 6−300 K at a field strength of 1 T using a Quantum Design MPMS SQUID magnetometer. The field dependence of the magnetization data from 0 to 5 T was measured at 6 and 80 K. The linear field dependence of the magnetization and zero-field intercept of 2×10^{-5} emu indicates the presence of no significant magnetic impurities. The susceptibility data were corrected for the sample container and the estimated core diamagnetism, -1.02×10^{-4} emu.

Results and Discussion

Synthesis. Solvothermal reaction conditions are invaluable for crystal growth and the synthesis of many new solid-state compounds. In addition to the enhanced solublizing and transport capacity of a supercritical or near-supercritical solvent, the molecules of solvent often stabilize voids in the formed crystalline networks. Water, the most commonly utilized solvothermal solvent, readily performs functions as both solvent and lattice solvate. Another dimension to solvothermal synthetic possibilities includes exploitation of the reactivity of the solvent and reactants. We previously reported the use of superheated acetonitrile as both a solvent and a dehydrating agent in the synthesis of the three-dimensional network of anhydrous β-$Mn(OAc)_2$.[8] The dehydrating ability of acetonitrile takes advantage of the fact that, under the solvothermal conditions, acetonitrile can react with 2 equiv of water to yield ammonia and acetic acid (eq 1) or ammonium acetate, recognizing the relative acid/base equilibrium. An anionic triacetate species of manganese (an as yet unknown species based on a search of the chemical abstracts) is not formed even in the presence of the excess ammonium acetate.

$$MeCN + 2H_2O \rightarrow NH_3 + MeCO_2H \qquad (1)$$

In an effort to expand the utility of this solvothermal dehydration reaction, we explored the solvothermal reaction of $MnCl_2 \cdot 4H_2O$ in acetonitrile. Under solvothermal reaction conditions, the manganese chloride is dehydrated, the 4 equiv of water yielding 2 equiv of ammonium acetate per 1 equiv of the tetrahydrate starting material. However, unlike the dehydration of manganese acetate hydrate, 1 equiv of ammonium acetate is added to the manganese chloride, forming the one-dimensional chain structure of $[NH_4]MnCl_2(OAc)$, **I**, upon dehydration and condensation, instead of forming anhydrous $MnCl_2$.

(6) Gabe, E. J.; Le Page, Y.; Charland, J.-P.; Lee, F. L.; White, P. S. *J. Appl. Crystallogr.* **1989**, *22*, 384.

(7) Jensen, S. J. *Acta Chem. Scand.* **1968**, *22*, 647.

(8) Martin, J. D.; Hess, R. F. *Chem. Commun.* **1996**, 2419.

Table 1. Summary of the Crystallographic Data

	I	II
formula	$[NH_4]MnCl_2(OAc)$	$[NH_4]_2MnCl_4 \cdot 2H_2O$
formula weight	202.92	268.85
temp, °C	20	20
space group	*C*2/*c* (No. 15)	*I*4/*mmm* (No. 139)
a, Å	15.191(6)	7.5250(5)
b, Å	7.044(2)	
c, Å	13.603(6)	8.276(2)
β, deg	107.31(4)	
V, Å^3	1389.7(9)	468.6(1)
Z	8	2
ρ_{calc}	1.940	1.905
λ, Å	0.710 73 (Mo Kα)	0.710 73 (Mo Kα)
μ, mm^{-1}	2.52	2.49
R^a	0.041	0.040
$R_w{}^b$	0.047	0.049

^{a} $R = \sum||F_o| - |F_c||/\sum|F_o|$. ^{b} $R_w = \sum(|F_o| - |F_c|)^2/\sum|F_o|^2$.

Related reactions were performed using the manganese chloride tetrahydrate starting material in the presence of additional poly(carboxylic acid)s in an attempt to form metal carboxylate networks. Under these conditions with oxalic acid, or 1,3,5-triazine, an approximately 15% yield of the hydrated salt, $[NH_4]_2MnCl_4 \cdot 2H_2O$, **II**, was observed, along with a reduced yield of **I** and an as yet unidentified carboxylate-containing species. These results suggest that more acidic reaction conditions reduce the dehydrating efficiency of the superheated acetonitrile.

Structure and Bonding. A summary of the crystallographic data for the single-crystal structures of $[NH_4]MnCl_2(OAc)$, **I**, and $[NH_4]_2MnCl_4 \cdot 2H_2O$, **II**, is given in Table 1. Full details of the structure solutions are available in the Supporting Information.

$[NH_4]MnCl_2(OAc)$, I. The structure of **I** exhibits chains of manganese chloride acetate that run along the crystallographic *b* axis as shown in Figure 1. The bidentate acetate ligands force this structure to be intermediate between the two classic structure types of an ABX_3 face-shared octahedral chain, such as $[NMe_4]MnCl_3$,[9] and the edge-shared octahedral chain of $[HNMe_3][MnCl_2(H_2O)_2][Cl]$.[10] In **I**, the manganese atoms reside along the 2_1 crystallographic axes with Mn−Mn separations of 3.52 Å. The acetate ligands symmetrically bridge between manganese atoms with Mn−O distances of 2.14 Å (average) and an Mn−O−C angle of 135° (average). The two nearly symmetrical chloride bridges are made distinct from each other by different hydrogen-bonding interactions with the ammonium cation. Cl(2), with the closest contact to the ammonium cation, exhibits the longest Mn−Cl(2) distances, 2.62 Å (average), whereas with less Cl- - -H hydrogen bonding, Mn−Cl(1) = 2.52 Å (average). This hydrogen-bond-induced elongation of the manganese chloride bonds is also reflected in the slightly smaller Mn−Cl(2)−Mn = 84.66(5)° bond angle as compared with Mn−Cl(1)−Mn = 88.55(5)°.

The ammonium cations sit in the troughs between neighboring acetate ligands with strong intrachain hydrogen bonds to the oxygen atoms of the acetate ligands, which fix the orientation of the tetrahedral $[NH_4]^+$ cations. The O(1)- - -H(3) = 2.04 Å and O(2)- - -H(1) = 2.01 Å contacts are coplanar but are tilted 12° out of the Mn−O−O−Mn plane. Much weaker intrachain Cl(1)- - -H(3) = 2.96 Å and Cl(1)- - -H(1) = 3.02 Å contacts are also observed. Hydrogens H(2) and H(4) are oriented orthogonal to the inorganic chain but form strong interchain H- - -Cl hydrogen bonds linking the chains in the *a* and *c* directions as shown in Figure 1b. The pair of strong Cl(2)- - -H(4) = 2.45 Å contacts with near-linear N−H(4)−Cl(2) = 171.4° hydrogen-bond contacts link neighboring chains along the *a* direction. This strong hydrogen bonding is also responsible for the above-mentioned lengthening of the Mn−Cl(2) bonds by about 0.1 Å. Hydrogen H(2) forms weaker hydrogen-bonded bridges between Cl(1) and Cl(2), with distances of 2.66 and 2.82 Å, respectively, linking neighboring chains along the *c* direction.

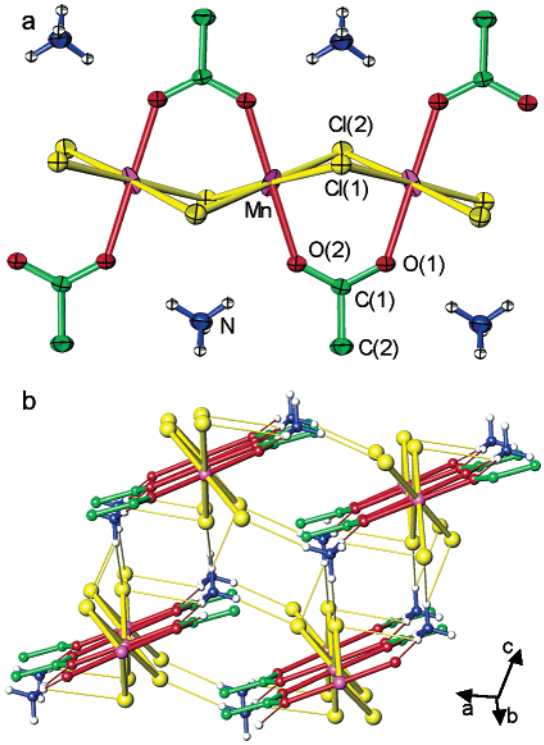

Figure 1. (a) ORTEP view of the one-dimensional chain of $[NH_4]MnCl_2(OAc)$, **I**, giving the atom labeling scheme. (b) Crystal packing diagram looking down the *b* axis. Hydrogen-bonding interactions between the ammonium cations and the acetate oxygen and chlorine atoms are drawn as red and yellow bonds, respectively.

$[NH_4]_2MnCl_4 \cdot 2H_2O$, II. The structure of **II** is isomorphous to the known crystal structure of $K_2MnCl_4 \cdot 2H_2O$,[7] which exhibits a body-centered tetragonal distribution of isolated $MnCl_4(OH_2)_2$ octahedra as shown in Figure 2. The water molecules are located on 4-fold axes; thus, the hydrogen positions are crystallographically disordered. The ammonium cations are oriented such that each hydrogen forms weak hydrogen bonds that bridge two edge chlorides of neighboring octahedra, NH- - -Cl = 2.70 Å and N−H- - -Cl = 135.87°. The primary difference between this structure with the ammonium cation and that of the previously reported potassium salt is a 0.11 Å expansion in the *a*/*b* lattice constants for the ammonium salt. This is inverse to the expected trend based on their relative ionic radii (NH_4^+ =

(9) Morrison, B.; Graeber, E. J. *Acta Crystallogr.* **1967**, *23*, 776.
(10) Caputo, R. E.; Willet, R. D.; Muir, J. *Acta Crystallogr.* **1976**, *B32*, 2639.

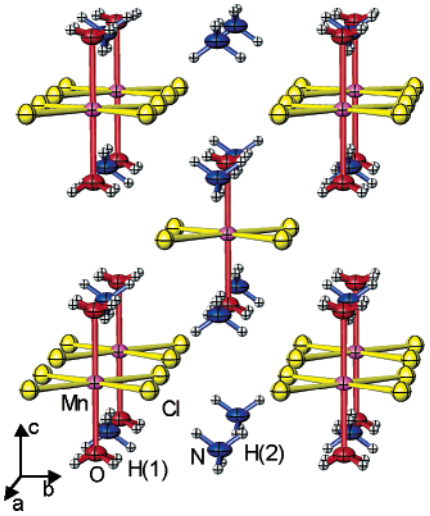

Figure 2. ORTEP plot indicating the crystal packing in the $[NH_4]MnCl_4(H_2O)_2$ salt, **II**.

1.51 Å[11] and K^+ = 1.52 Å (CN = 6) and 1.65 Å (CN = 8)[12]), suggesting that differential hydrogen bonding may be responsible for the subtle difference in structures. The intermolecular hydrogen bonding is dominated by the OH- - -Cl = 2.581 Å and O−H- - -Cl = 155.15° contacts, which are significantly longer in **II** than the analogous 2.470 Å and O−H- - -Cl = 174° contacts in the potassium salt (O−H distances from the reported crystal structure of the potassium salt were idealized to 0.86 Å for comparison). The NH- - -Cl hydrogen bonding from the ammonium cation, which is not available in the potassium salt, competes with the OH- - -Cl hydrogen bonding in **II**. However, the resultant net influence of the hydrogen bonding on Mn−Cl bonds is constant between the K^+ and NH_4^+ structures, consistent with the observed Mn−Cl Δd of only 0.013 Å, as compared to the Mn−Cl Δd of 0.11 Å observed as a result of the differential hydrogen bonding in **I**. However, the more indirect NH- - -$(Cl)_2$ hydrogen bonds to the octahedral edge do not compensate the lattice effects of the loss of the direct OH- - -Cl hydrogen bonds resulting in the expanded lattice for the ammonium salt.

Magnetism vs Structure. The magnetic susceptibility of **I** is plotted in Figure 3. Above 80 K, the data exhibit Curie−Weiss behavior with μ_{eff} = 6.09 μ_B, consistent with spin $S = {}^5/_2$Mn(II). Antiferromagnetic ordering is observed with a maximum in the susceptibility at 20 K, which is well fit by the Bonner−Fisher model for a Heisenberg antiferromagnet[13] with an intrachain exchange constant $J/k = -2.39$ K. Given that the expanded acetate ligand bridge in **I** results in a structure that can be described as intermediate between that of a face-shared μ_3-type and edge-shared μ_2-type (see Chart 1) octahedral chain, it is interesting that the magnitude of its exchange constant is about half that found for the μ_3 chains of $[A]MnCl_3$ (A = NMe_4^+ and $H_2NMe_2^+$), which have been exhaustively studied as "ideal" one-dimensional Heisenberg antiferromagnets,[14,15] and almost an order of magnitude greater than that found in the μ_2-type $[A]MnCl_2(H_2O)_2[Cl]$ (A = $HNMe_3^+$, $C_9H_7NH^+$, and Hpy^+) one-dimensional chains.[16−18] By contrast, the exchange constant in **I** is essentially equivalent to that observed for the μ_1-type $[A]MnCl_3(H_2O)_2$ (A = $H_2NMe_2^+$, H_3NMe^+, and Cs^+) chains.[19−21] These comparative data are summarized in Table 2.

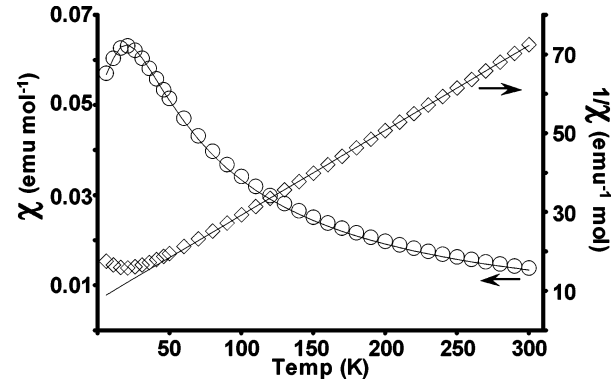

Figure 3. Plot of the magnetic susceptibility data (open circles) for **I**, fit to the Bonner−Fisher formalism (solid curve) with $J/k = -2.39$ K (left axis) and Curie−Weiss plot of $1/c$ vs T (open squares, right axis) with a linear regression fit (solid line) for data above 80 K (C = 4.65, $q = -35.63$).

Chart 1

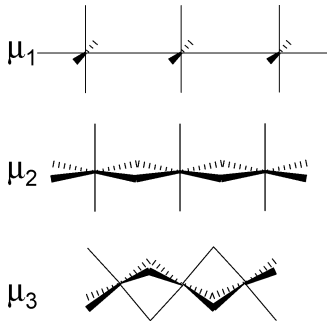

Common to each of these classes of chain compounds are the metal−chloride bridges, which provide the primary pathway for the magnetic superexchange. The metal−metal distances (see Table 2) are too great for any significant direct exchange, and furthermore, the increase in the magnetic exchange on going from μ_2 to μ_1 structures is inverse to what would be expected based on the respective distance between metal centers. The Mn−Cl distances, however, are essentially constant throughout this entire series of compounds, averag-

(11) Jenkins, H. D. B.; Thakur, K. P. *J. Chem. Educ.* **1979**, *56*, 576.
(12) Shannon, R. D.; Prewitt, C. T. *Acta Crystallogr.* **1969**, *B25*, 925.
(13) Carlin, R. L. *Magnetochemistry*; Springer-Verlag: New York, 1986; Chapters 6 and 7.
(14) Dingle, R.; Lines, M. E.; Holt, S. L. *Phys. Rev.* **1969**, *187*, 643.
(15) (a) Caputo, R. E.; Willett, R. D. *Phys. Rev. B* **1976**, *13*, 3956. (b) Takeda, K.; Schouten, J. C.; Kopinga, K.; deJonge, W. J. M. *Phys. Rev. B* **1978**, *17*, 1285.
(16) Merchant, S.; McElearney, J. N.; Shankle, G. E.; Carlin, R. L. *Physica* **1974**, *78*, 308.
(17) Caputo, R. E.; Willett, R. D.; Morosin, B. *J. Chem. Phys.* **1978**, *69*, 4976.
(18) Richards, P. M.; Quinn, R. K.; Morosin, B. *J. Chem. Phys.* **1973**, *59*, 4474.
(19) (a) Caputo, R. E.; Willett, R. D. *Acta Crystallogr.* **1981**, *B37*, 1618. (b) Boersma, F.; Tinus, A. M. C.; Kopinga, K.; Paduan-Filho, A.; Carlin, R. L. *Physica* **1982**, *B114*, 231.
(20) (a) Caputo, R. E.; Willett, R. D. *Acta Crystallogr.* **1981**, *B37*, 1616. (b) Simizu, S.; Chen, J.-Y. Friedberg, S. A. *J. Appl. Phys.* **1984**, *55*, 2398.
(21) Kobayashi, H.; Tsujikawa, I.; Friedberg, S. A. *J. Low Temp. Phys.* **1973**, *10*, 62.

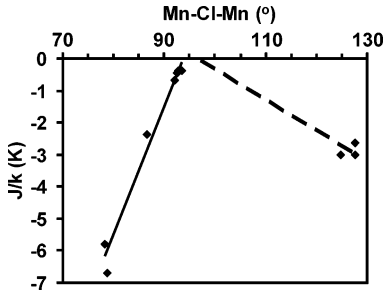

Figure 4. Plot of the exchange coupling (J/k) vs the Mn−Cl−Mn bond angle, α, for the series of chloride-bridged manganese chains described in Table 2. The solid line is the linear fit to the acute-angle ligand-bridged data for μ_2- and μ_3-type chains, suggesting a special angle $\alpha = 93.7°$ for acute-angle ligand bridges where $J = 0$. The dashed line corresponds to the linear fit to the assumed special angle of 97.5° for obtuse-angle ligand bridges and the observed data for μ_1-type chains.

Table 2. Structure versus Intrachain Magnetic Coupling in Chloride-Bridged Manganese One-Dimensional Chains

compound	type	Mn−Mn (Å)	Mn−Cl−Mn (average) (deg)	J/k (K)	ref
$[H_2N(Me)_2]MnCl_3(H_2O)_2$	μ_1	4.67	127.60	−2.65	19
$[H_3NMe]MnCl_3(H_2O)_2$	μ_1	4.60	127.58	−3.01	20
$CsMnCl_3(H_2O)_2$	μ_1	4.55	124.78	−3.0	21
$[HN(Me)_3]MnCl_2(H_2O)_2[Cl]$	μ_2	3.72	93.48	−0.36	10 and 16
$[C_9H_7NH]MnCl_2(H_2O)_2[Cl]$	μ_2	3.70	92.78	−0.36	17
$MnCl_2(H_2O)_2$	μ_2	3.69	92.55	−0.45	22
$MnCl_2(py)_2$	μ_2	3.7	~93	−0.59	18
$[Hpy]MnCl_2(H_2O)_2[Cl]$	μ_2	3.67	92.16	−0.69	17 and 18
$[NH_4]MnCl_2(OAc)$	μ_2/μ_3	3.52	86.58	−2.39	this work
$[NMe_4]MnCl_3$	μ_3	3.25	78.69	−6.7	14
$[H_2NMe_2]MnCl_3$	μ_3	3.23	78.37	−6.9 or −5.8	15

ing about 2.55 Å. The primary role of the chlorine bridges in the superexchange is further exemplified by the minimal variation in the exchange constants of $[A]MnCl_2(H_2O)_2[Cl]$ ($A = HNMe_3^+$, $C_9H_7NH^+$, and Hpy^+), $MnCl_2(H_2O)_2$,[22] and $MnCl_2(py)_2$,[18] which all adopt μ_2-type structures. None of the changes in the ancillary ligands or cations have a major impact on the intrachain exchange coupling (Table 2), although they do impact the weaker interchain coupling. The acetate ligand in **I** similarly appears to play a minor role in the intrachain coupling, consistent with previous reports of acetate ligands only weakly mediating magnetic exchange as compared to a single atom bridge.[23] The greater superexchange through chlorine is, in part, explained by its lower electronegativity and more diffuse orbitals than those found for the acetate oxygens. Interestingly, there is a systematic linear correlation between the Mn−Cl−Mn bond angle, α, and the intrachain exchange constant J, as shown in Figure 4. Compound **I**, with $\alpha = 87°$, is a missing link between the μ_3-type chains with $\alpha \approx 79°$ and the μ_2-type chains with $\alpha \approx 92°$. This linear relationship for acute values of α, given by eq 2, implies that J should go to 0 at $\alpha = 93.6°$. This result is complementary to the linear relationship reported by Hatfield and Hodgson for hydroxo-bridged copper(II) dimers with obtuse values of α.[24] In the latter work, $J = 0$ was predicted to occur at $\alpha = 97.5°$.

$$J/k = (0.40\ \text{K/deg})\alpha - 38\ \text{K} \qquad (2)$$

The angular dependence of the intrachain exchange coupling in the octahedral manganese(II) chains can be qualitatively traced to the e_g-type metal−ligand σ^* interactions, similar to that described for the magnetic superexchange in square-planar copper dimers,[25] by using a spin-dimer approach to extended systems.[26] The primary path for superexchange with acute-angle bridges, such as that observed for the μ_3-type chains, utilizes the chlorine orbital of type A_s, sketched below.

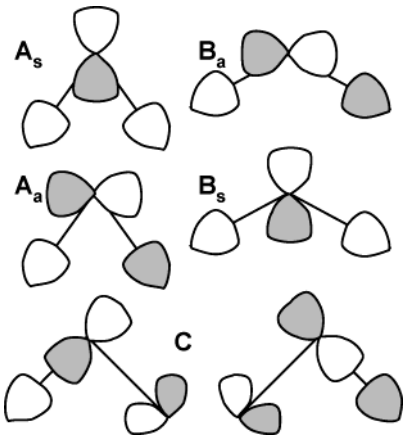

By contrast, the antisymmetric orbital of type B_a will provide the primary path for superexchange for obtuse-angle bridges. In the case of the acute-angle bridge, the symmetric A_s interaction will be destabilized with respect to the antisymmetric A_a, which results in the stabilization of the spin-dimer singlet, antiferromagnetic ground state. A spin-dimer singlet, antiferromagnetic ground state will similarly be observed for structures with obtuse-angle bridges in which B_a is destabilized with respect to B_s. The Δe between symmetric and antisymmetric interactions, which directly correlates to the square root of the exchange constant,[26] therefore must reach a minimum for some intermediate bond angle α near 90°.[25] At this special angle where Δe is at a minimum, there will be little superexchange, with the linear combination of atomic orbitals shown in C giving at best weak σ^*/π^*-type superexchange. In this region the spin-dimer triplet will be the ground state, thus giving rise to ferromagnetic exchange.

While the hydroxide-bridged d^9 Cu(II) dimers are very different from the chloride-bridged d^5 Mn(II) chains, and thus one must be cautious regarding overinterpretation, the octahedral manganese system seems to provide experimental confirmation of the theoretical predictions for superexchange through acute-angle ligand bridges[25] that were based on the experimental copper system.[24] A spin dimer of $S = {}^5/_2$Mn-

(22) McElearney, J. N.; Merchant, S.; Carlin, R. L. *Inorg. Chem.* **1973**, *12*, 906.
(23) McKee, V.; Zvagulis, M.; Reed, C. A. *Inorg. Chem.* **1985**, *24*, 2914.
(24) Crawford, W. H.; Richardson, H. W.; Wasson, J. R.; Hodgson, D. J.; Hatfield, W. E. *Inorg. Chem.* **1976**, *15*, 2107.
(25) Hay, P. J.; Thibeault, J. C.; Hoffmann, R. *J. Am. Chem. Soc.* **1975**, *97*, 4884.
(26) Whangbo, M.-H.; Koo, H.-J.; Dai, D. *J. Solid State Chem.* **2003**, *176*, 417.

(II) is expected to exhibit J coupling of at least 25 times less than a spin dimer of $S = {}^1/_2$Cu(II). However, special angles where $J/k = 0$ of $\alpha = 93.6°$ based on acute-bridged systems described in this work and $\alpha = 97.5°$ based on obtuse-bridged systems described by Hodges and Hatfield[24] suggests a small range of ligand-bridged angles where intrachain ferromagnetic coupling may be observed. Ferromagnetic coupling is, in fact, observed in the copper(II) system for $97.5° > \alpha > 95.6°$.[24] The limited set of data for the μ_1-type Mn(II) chains listed in Table 2 shows increased antiferromagnetic exchange constants for structures with obtuse-angle ligand bridges. If the obtuse-angle limit is assumed to be 97.5°, based on the copper hydroxide system, then using the exchange constant data of the μ_1-type chains, the linear relationship shown by the dashed line in Figure 4 [$J/k = (-0.0977$ K/deg)$\alpha + 9.50$ K] offers a prediction for the antiferromagnetic exchange constants of additional Mn(II) chains.

Conclusions

The synthetic utility of the solvothermal dehydration reaction using superheated acetonitrile has been demonstrated with the synthesis of two new manganese chloride salts. The complete dehydration of $MnCl_2 \cdot 4H_2O$ in superheated acetonitrile was achieved in the formation of $[NH_4]MnCl_2(OAc)$, **I**. By contrast, incomplete dehydration was achieved in the presence of weak acids, resulting in the formation of $[NH_4]_2MnCl_4(H_2O)_2$, **II**. Extensive hydrogen bonding between the ammonium cations and the complex anions exhibits significant control over both the local Mn−Cl bonding and the lattice organization of these salts.

Magnetic susceptibility measurements of **I** show it to nicely fit the Bonner−Fisher model for a Heissenberg antiferromagnet with an exchange constant $J/k = -2.39$ K. The magnitude of this magnetic exchange is intermediate between that of two classic one-dimensional Heissenberg antiferromagnetic systems with two or three chloride bridges. A comparison of the structural and magnetic behavior of a series of chloride-bridged octahedral Mn(II) chains demonstrates a linear correlation between the Mn−Cl−Mn bond angle and the magnitude of the intrachain exchange constant. This work provides the complementary structure/property correlations for acute-angle ligand-bridged systems for comparison with previously assembled data for obtuse-angle ligand-bridged copper dimers, giving a more complete understanding of the structural and ligand orbital effects on magnetic superexchange.

Acknowledgment. Support for this work via Contracts NSF DMR-9501370 and DMR-0305086 is gratefully acknowledged. Magnetic susceptibility data were collected by J. Ostensen at Iowa State University. J.D.M. is a Cottrell Scholar of the Research Corp.

Supporting Information Available: X-ray crystallographic data for **I** and **II** are available in CIF format. This material is available free of charge via the Internet at http://pubs.acs.org.

IC049881R